

Intuitive Exposition of Third Order Surface Behavior



*Pushkar Prakash Joshi
Carlo H. Séquin*

Electrical Engineering and Computer Sciences
University of California at Berkeley

Technical Report No. UCB/EECS-2008-125
<http://www.eecs.berkeley.edu/Pubs/TechRpts/2008/EECS-2008-125.html>

September 25, 2008

Copyright 2008, by the author(s).
All rights reserved.

Permission to make digital or hard copies of all or part of this work for personal or classroom use is granted without fee provided that copies are not made or distributed for profit or commercial advantage and that copies bear this notice and the full citation on the first page. To copy otherwise, to republish, to post on servers or to redistribute to lists, requires prior specific permission.

Intuitive Exposition of Third Order Surface Behavior

Pushkar Joshi¹ and Carlo Séquin²

¹ppj@eecs.berkeley.edu, ²sequin@eecs.berkeley.edu
C.S. Division, University of California, Berkeley

September 18, 2008

Abstract

Third order surface analysis is an important aspect of shape interrogation and design. We present a novel parameterization-independent exposition of the geometric behavior of a surface point up to third order. Unlike existing algebraic expositions, our work produces an intuitive explanation of the third order surface behavior, analogous to the principal curvatures and directions that describe second order behavior. We extract four parameters that provide a quick and concise understanding of the third order surface behavior at any given point. Our shape parameters can be used to characterize different third order surface shapes without having to use tensor algebra.

1 Introduction

Surface analysis (also known as shape interrogation) is a useful tool for understanding the geometric behavior of a surface near a given point. In the general case of a smooth surface, one can analyze the geometry up to a given order by performing a Taylor expansion of the surface near a given point. As an example, the zeroth order surface analysis yields the position of that point. The first order analysis adds the tangent plane, the second order the curvature tensor, and the third order a rank-3 tensor that describes the derivatives of curvature. The higher the order of surface analysis, the more information about the shape is extracted.

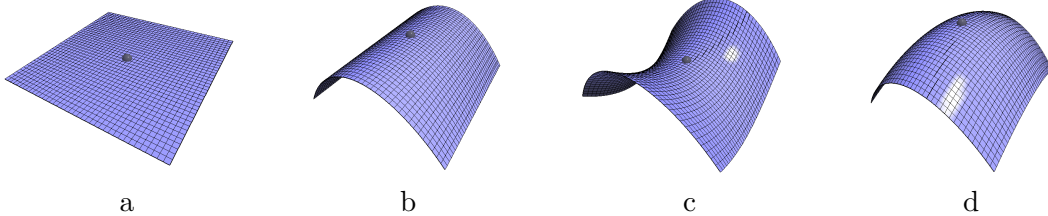


Figure 1: Up to second order, we can intuitively classify a surface point as (a) flat, (b) parabolic, (c) hyperbolic, and (d) elliptic.

Surface analysis using Taylor expansion produces shape information that is compactly stored in tensors. Extracting this information from the tensors requires us to formulate an input query in the tensor's coordinate system. For instance, in order to compute the normal curvature in a given direction at a surface point, we first express the direction as a vector in the point's tangent plane, provide the same vector as both inputs to the quadratic, second fundamental form (a rank-2 curvature tensor), and re-scale the result by the area metric (multiply by the inverse of the first

fundamental form). We perform a similar sequence of operations to extract various derivatives of surface curvature; we need to provide three directions to the rank-3 tensor that encapsulates the curvature derivative information. Extracting precise shape information at a surface point thus requires us to understand how to query the shape tensors at that point.

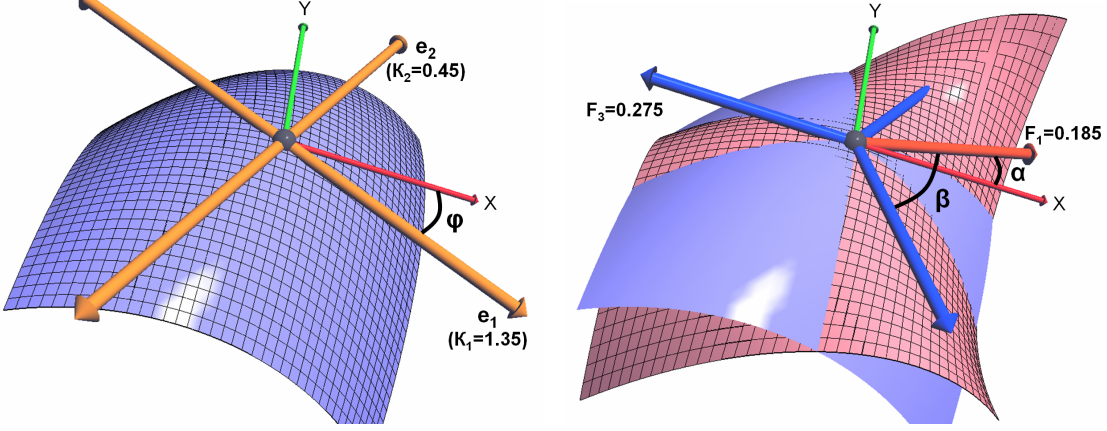


Figure 2: **Left:** Second order frame comprised of principal directions and their associated principal curvatures. The angle ϕ indicates the rotation of the frame from the user provided x -axis. The entire second order behavior is described by three numbers: κ_1 , κ_2 and ϕ .

Right: Third order frame comprised of four directions: one indicating the peak of the first Fourier component and the other three indicating equally spaced peaks of the third Fourier component. Angle α indicates the rotation of the frame from the user provided x -axis, and angle β indicates the rotation of the third Fourier component from the first Fourier component. The entire third order behavior is described by four numbers: F_1 , F_3 , α and β . The cubic surface in pink is super-imposed on the original quadratic surface in blue to show the undulatory third order behavior. All directions are in the tangent plane of the point.

However, most people, in particular novices to linear algebra, are more apt to extract shape information from simple geometric primitives. For instance, up to second order we can easily classify a surface point as flat, elliptic, hyperbolic or parabolic (see Fig. 1), without having to query the curvature tensor. We can perform this intuitive classification by focusing on the principal curvatures κ_1 and κ_2 . When the product $\kappa_1\kappa_2$ (also known as the Gaussian curvature) is positive, negative, or zero, the surface is elliptic, hyperbolic, or parabolic, respectively. In the special case where κ_1 and κ_2 are equal, the surface point is umbilic. Of course, when both κ_1 and κ_2 are zero, the surface is flat. Euler's theorem tells us that the principal directions (e_1 and e_2) corresponding to the principal curvatures (κ_1 and κ_2 respectively) are mutually orthogonal. Therefore, we can completely describe the second order shape of a surface point by three intuitive parameters: the two principal curvatures (κ_1 and κ_2) and the angle ϕ made by the e_1 principal direction with an arbitrary direction in the tangent plane (see Fig. 2). These three parameters encapsulate exactly the same information as that in the second fundamental form, but are more accessible to novices and to visual and geometrical thinkers. We believe that this geometrical analysis results in a more intuitive and widespread understanding of second order shape behavior.

For many surface design tasks, geometric analysis only up to second order is not sufficient because it ignores a significant amount of shape behavior. Therefore, we need to study and understand higher order shape behavior. As one step towards that goal, we focus on third order analysis. We have not been able to find an intuitive description for third order surface behavior in the literature.

Most of the third order shape knowledge is expressed using the algebra of rank-3 tensors. As a result, a thorough understanding of third order surface behavior is typically limited to those people who are comfortable with tensor algebra.

Contribution In this report, we provide an intuitive, geometric description of third order surface behavior. Our description is similar in its intuitive nature to the readily accessible second order description using principal curvatures and directions. We extract four shape parameters that completely describe the third order shape behavior at a surface point. Our shape parameters are independent of any coordinate system and are obtained by decomposing the third order shape function into its Fourier components.

2 Previous Work

While not as commonly studied as second order surface behavior, third order surface behavior has been studied for selective applications. In computer graphics, the most common application is to convey shape information via line drawings such as suggestive contours [2] or other salient mesh features [10]. Rusinkiewicz [9] describes how the construction of the rank-3 tensor can be used to interrogate the derivatives of normal curvature in arbitrary directions. These curvature derivatives provide shape information that is perceptually important to the visual system. While the rank-3 tensor yields precise curvature derivative information, it does not provide an easy-to-understand qualitative description of the third order shape information.

In computer-aided geometric design, third order surface energies are optimized to produce smooth surfaces. Moreton and Séquin [7] introduced the “Minimum Variation Surface” (MVS) energy that minimizes the derivatives of principal curvatures along the respective principal directions, and Joshi and Séquin [4] enhanced the original MVS formulation by adding cross derivative terms. Mehlum and Tarrou [6] formulated a more complete energy by measuring inline normal curvature variation over all directions at a surface point; Gravesen and Ungstrup [3] further enhanced the work of Mehlum and Tarrou by considering curvature variation for all surface curves (not just normal section curves). Gu and Zhang [11] minimize the variation of mean curvature of a surface by solving the corresponding (sixth order) Euler-Lagrange equation.

Designing such energies typically requires understanding some aspect of third order surface behavior. For instance, Mehlum and Tarrou [6] formulate an expression that provides the arc-length derivative of the normal curvature in a given direction. They introduce four parameterization-dependent third order shape parameters, P, Q, S, T . These terms essentially encode the normal components of parametric surface derivatives. While useful for computing the energy values, these parameters do not easily provide a qualitative description of the third order shape at a given point.

Umbilic points (surface points with equal principal curvatures) have received a special amount of third order analysis — understanding the behavior of a surface near umbilics is useful for manufacturing thin shell parts [5] and studying geometrical optics [1]. As a result, numerous researchers have explored the exact geometric nature of umbilic points. A common method of characterizing an umbilic point is Darboux’s classification according to the pattern of lines of curvature near the point (*star*, *monstar* and *lemon* — see [1] for a visual description and [8] for a detailed description). Maekawa et al. [5] analyze the local surface geometry near an umbilic point in order to compute curvature lines that pass through that point. The initial setup for the surface analysis near the umbilic point is similar to ours, but further analysis focuses on the umbilic classification and lacks the intuitive, qualitative description we seek.

In a nutshell, previously, researchers have extensively studied specific aspects of third order

surface behavior corresponding to particular applications, but an *intuitive, purely geometric description is missing*. Informally speaking, the “algebra of third order behavior” has been studied sufficiently; the “geometry of third order behavior” needs to be brought up to a corresponding level of understanding. We hope that the following exposition serves as a significant step towards that goal.

3 Third Order Parameters for Polynomial Height Field

In order to introduce the intuition behind the necessary mathematical concepts, we will initially focus our attention on an idealized, smooth surface patch centered at a given point. Consider the surface near a point that is described fully by a height field above the tangent plane at that point: a function of the two independent variables x and y :

$$\begin{aligned} z(x, y) = & C_0x^3 + C_1y^3 + C_2x^2y + C_3xy^2 \\ & + Q_0x^2 + Q_1y^2 + Q_2xy \\ & + L_0x + L_1y + K \end{aligned} \tag{1}$$

We will assume that the directions corresponding to x and y are mutually orthogonal and that first order and constant parameters (L_0, L_1, K) are zero. This assumption is an over-simplification and is not valid for a general surface patch. However, we found it easier to first develop an intuition for the third order parameters using this idealized patch. In Section 6 we describe how to extract the third order shape parameters for a general surface patch.

As a first step, we convert the cubic height function $z(x, y)$ into polar coordinates $z_p(r, \theta)$, where $r = \sqrt{x^2 + y^2}$ and $\theta = \tan^{-1}(y/x)$. We then extract the parameters affecting only the second (quadratic) and third (cubic) order behavior of the surface into separate equations:

$$z_{pq}(r, \theta) = r^2[Q_0 \cos^2 \theta + Q_1 \sin^2 \theta + Q_2 \cos \theta \sin \theta] \tag{2}$$

$$z_{pc}(r, \theta) = r^3[C_0 \cos^3 \theta + C_1 \sin^3 \theta + C_2 \cos^2 \theta \sin \theta + C_3 \cos \theta \sin^2 \theta] \tag{3}$$

Previous work follows a similar setup up to this step. At this point, people solve for the extremal values of θ by solving the quadratic equation $\frac{dz_{pq}(r, \theta)}{d\theta} = 0$ and cubic equation $\frac{dz_{pc}(r, \theta)}{d\theta} = 0$ (e.g. see [6], [5]). The roots of the quadratic equation yield the principal curvature directions. The number of real roots of the cubic equation (1 or 3) and their distribution with respect to each other is used to classify umbilic points or to study maxima of curvature variation. We have obtained a more intuitive understanding of the third order behavior by decomposing the functions z_{pq} and z_{pc} into their Fourier components.

4 Fourier Analysis of Quadratic Height Function

As an introductory exercise, we analyze the Fourier components of the quadratic height function and show how the amplitudes and phase shifts of the Fourier components yield the well-known second order shape parameters. The Fourier components of the functions that comprise $z_{pq}(r, \theta)$ can easily be extracted:

$$\cos^2 \theta = 0.5 + 0.5 \cos 2\theta \tag{4}$$

$$\sin^2 \theta = 0.5 - 0.5 \cos 2\theta \tag{5}$$

$$\cos \theta \sin \theta = 0.5 \sin 2\theta \tag{6}$$

Therefore, z_{pq} can be expressed as a constant term plus a linear combination of the Fourier components $\cos 2\theta$ and $\sin 2\theta$, which can be further simplified as an equation using a single phase-shifted cosine function. That is,

$$z_{pq}(r, \theta) = r^2[F_0 + F_2 \cos(2(\theta + \phi))] \quad (7)$$

where F_0 represents the mean value of z_{pq} , and F_2 represents the amplitude of the cosine component that gets added to the mean. The cosine term is a symmetric function that produces four equally spaced extremal values in the range $[0, 2\pi]$. The maxima and minima correspond to the well-known principal curvatures and the mutually orthogonal principal directions. The angle ϕ is the phase shift that is computed with respect to an arbitrary, user-provided direction (usually the x -axis or the u -direction). Therefore, the entire second order shape information can be compactly described in a parameterization-independent manner by three terms (F_0 , F_2 and ϕ). By computing $\kappa_1 = F_0 + F_2$ and $\kappa_2 = F_0 - F_2$ we get the three familiar terms: κ_1 , κ_2 , ϕ .

5 Fourier Analysis of Cubic Height Function

Similar to the quadratic height function, we extract the Fourier components of the functions that make up $z_{pc}(r, \theta)$:

$$\cos^3 \theta = 0.75 \cos \theta + 0.25 \cos 3\theta \quad (8)$$

$$\sin^3 \theta = 0.75 \sin \theta - 0.25 \sin 3\theta \quad (9)$$

$$\cos^2 \theta \sin \theta = 0.25 \sin \theta + 0.25 \sin 3\theta \quad (10)$$

$$\cos \theta \sin^2 \theta = 0.25 \cos \theta - 0.25 \cos 3\theta \quad (11)$$

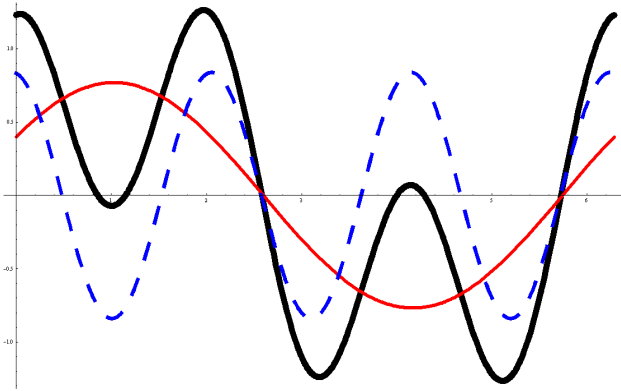


Figure 3: Third order height function from Eqn. 3 (thick black) is a sum of two cubic sinusoidal height functions: $\cos \theta$ (solid red) and $\cos 3\theta$ (dashed blue)

The cubic shape function z_{pc} can then be expressed as a linear combination of two Fourier components, $\cos \theta$ and $\cos 3\theta$:

$$z_{pc}(r, \theta) = r^3[F_1 \cos(\theta + \alpha) + F_3 \cos(3(\theta + \delta))] \quad (12)$$

where F_1 and F_3 are the amplitudes of the Fourier components, and α and δ are the phase shifts from an arbitrary, user-provided direction (the x -axis in our case). Fig. 3 illustrates this linear combination for a fixed value of r . Fig. 4 illustrates the combination of these Fourier components to form the cubic surface.

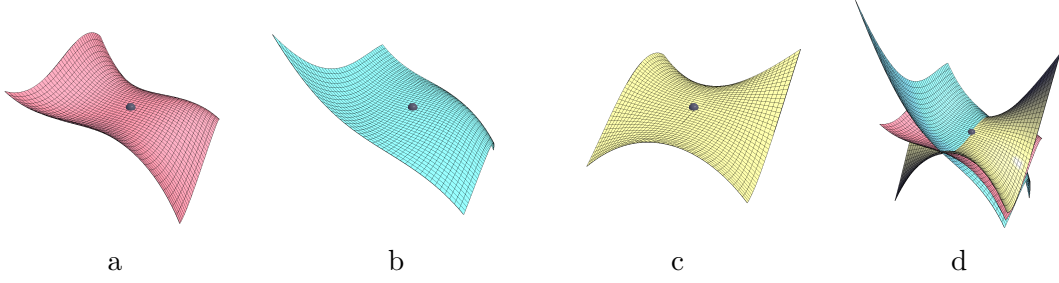


Figure 4: The third order surface is a combination of two sinusoidal functions ($\cos\theta$ and $\cos 3\theta$) which are the Fourier components of the third order shape function. We show (a) the original cubic surface, (b) only the first Fourier component, (c) only the third Fourier component, and (d) the original cubic surface sandwiched between constituent Fourier components with twice their original amplitudes. (d) clearly shows that the cubic surface is the average of the twice the Fourier components, and therefore is equal to the sum of the Fourier components.

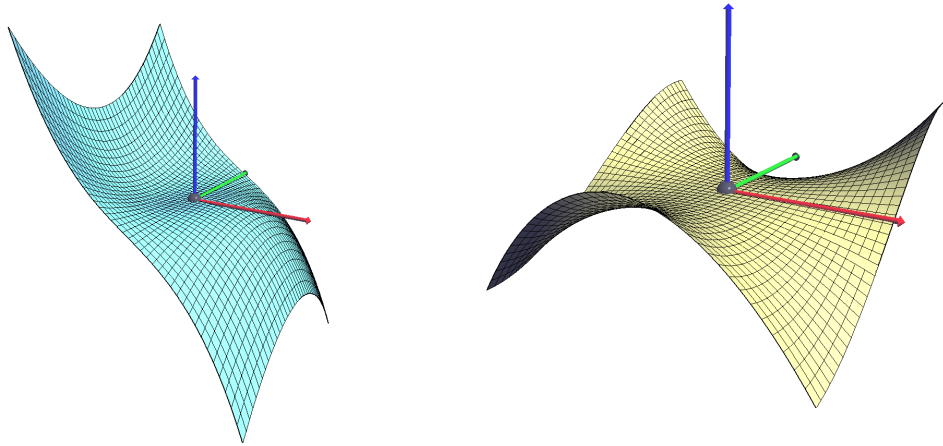


Figure 5: The first and third Fourier components of the third order shape function — all third order surface behavior can be expressed as properly scaled and rotated combinations of these two shapes.

We can consider the two phase shifts α and δ independently of each other. However, we found it more instructive to consider the direction corresponding to the (single) maximum of $F_1 \cos(\theta + \alpha)$ as a “third order principal direction”. Then, the phase shift δ can be expressed as $\alpha + \beta$, where β is the phase shift with respect to the third order principal direction. Therefore, we get our final equation for describing the cubic behavior of the surface:

$$z_{p_c}(r, \theta) = r^3[F_1 \cos(\theta + \alpha) + F_3 \cos(3(\theta + \alpha + \beta))] \quad (13)$$

We use the terms from Eqn. 13 as our four parameterization-independent, geometrically intuitive shape parameters (illustrated in Fig. 2). These parameters can easily be extracted from the original

third order parameters C_0, C_1, C_2, C_3 (Eqn. 3) of the polynomial height field:

$$F_1 = \frac{\sqrt{(3C_0 + C_3)^2 + (3C_1 + C_2)^2}}{4} \quad (14)$$

$$F_3 = \frac{\sqrt{(C_0 - C_3)^2 + (C_2 - C_1)^2}}{4} \quad (15)$$

$$\alpha = \tan^{-1} \left(\frac{3C_1 + C_2}{3C_0 + C_3} \right) \quad (16)$$

$$\beta = \frac{1}{3} \tan^{-1} \left(\frac{C_2 - C_1}{C_0 - C_3} \right) - \alpha \quad (17)$$

Similarly, given our third order parameters F_1, F_3, α and β , we can extract the parameterization-dependent third order parameters for the idealized surface patch:

$$C_0 = F_1 \cos(\alpha) + F_3 \cos(\beta) \quad (18)$$

$$C_1 = F_1 \sin(\alpha) - F_3 \sin(\beta) \quad (19)$$

$$C_2 = F_1 \sin(\alpha) + 3F_3 \sin(\beta) \quad (20)$$

$$C_3 = F_1 \cos(\alpha) - 3F_3 \cos(\beta) \quad (21)$$

6 Computing Fourier Components for a General Surface Patch

In this section we describe how to compute the third order shape parameters for a point on a general surface patch. Unlike the approach taken in Section 3, we can no longer ignore the effect of low order shape parameters (namely: first order and second order parameters) on the third order shape parameters. Therefore, we cannot extract parameterization independent shape parameters simply by analyzing a polynomial height field. Instead, we need to perform a Fourier analysis of the function that denotes the arc-length derivative of normal curvature. The Fourier coefficients can then be combined as above to yield the required shape parameters.

Consider that we have a bi-variate tensor product surface patch (e.g. a bi-cubic b-spline patch) parameterized by u, v . Given a point (u, v) in parameter space, let $\mathbf{S}(u, v)$ denote the 3D position of the point, \mathbf{n} denote the unit normal, and $\mathbf{S}_u(u, v), \mathbf{S}_v(u, v), \mathbf{S}_{uu}(u, v)$, etc. denote the 3D parametric surface derivatives with respect to u and v . Our task is to efficiently and exactly compute the F_1, F_3, α and β parameters for any point u, v on the patch.

First, compute the parameterization-dependent third order shape parameters P, Q, S , and T introduced by Mehlum and Tarrou [6]:

$$P = \mathbf{S}_{uuu} \cdot \mathbf{n} + 3\mathbf{S}_{uu} \cdot \mathbf{n}_u \quad (22)$$

$$Q = \mathbf{S}_{uuv} \cdot \mathbf{n} + 2\mathbf{S}_{uv} \cdot \mathbf{n}_u + \mathbf{S}_{uu} \cdot \mathbf{n}_v \quad (23)$$

$$S = \mathbf{S}_{uvv} \cdot \mathbf{n} + 2\mathbf{S}_{uv} \cdot \mathbf{n}_v + \mathbf{S}_{vv} \cdot \mathbf{n}_u \quad (24)$$

$$T = \mathbf{S}_{vvv} \cdot \mathbf{n} + 3\mathbf{S}_{vv} \cdot \mathbf{n}_v \quad (25)$$

Then, use the formula from [6] that expresses the arc-length derivative of normal curvature as a function of the angle θ from any given reference direction:

$$\begin{aligned} \kappa'_n(\theta) = & \frac{1}{\sigma^3} [PG^{3/2} \sin^3(\theta) + 3QGE^{1/2} \sin^2(\theta) \cos(\theta + \psi) \\ & + 3SEG^{1/2} \sin(\theta) \cos^2(\theta + \psi) + TE^{3/2} \cos^3(\theta + \psi)] \end{aligned} \quad (26)$$

where θ is measured from the u direction, E , F and G are coefficients of the first fundamental form (the metric tensor), and $\sigma = \sqrt{F^2 - EG}$ is the area element at the point of analysis. ψ denotes the complement to the angle between the u and v directions and is given by $\tan(\psi) = F/\sqrt{EG}$. (In the polynomial height field setup of Section 3, the coordinate axes were mutually orthogonal and therefore ψ was zero.)

Eqn. 26 can be written as an expression similar to Eqn. 3:

$$\kappa'_n(\theta) = A \cos^3(\theta + \psi) + B \sin^3(\theta) + C \sin(\theta) \cos^2(\theta + \psi) + D \sin^2(\theta) \cos(\theta + \psi) \quad (27)$$

where the coefficients A , B , C , and D can easily be written as functions of P , Q , S , T and E , F , G :

$$A = \frac{TE^{3/2}}{\sigma^3}, \quad B = \frac{PG^{3/2}}{\sigma^3} \quad (28)$$

$$C = \frac{3SEG^{1/2}}{\sigma^3}, \quad D = \frac{3QGE^{1/2}}{\sigma^3} \quad (29)$$

As described in Section 5, we can perform a Fourier analysis of the sinusoidal functions in Eqn. 27:

$$\begin{aligned} \cos^3(\theta + \psi) &= 0.75 \cos(\psi) \cos(\theta) - 0.75 \sin(\psi) \sin(\theta) \\ &\quad + 0.25 \cos(3\psi) \cos(3\theta) - 0.25 \sin(3\psi) \sin(3\theta) \end{aligned} \quad (30)$$

$$\sin^3(\theta) = 0.75 \sin(\theta) - 0.25 \sin(3\theta) \quad (31)$$

$$\begin{aligned} \cos^2(\theta + \psi) \sin(\theta) &= -0.25 \sin(2\psi) \cos(\theta) - 0.25(\cos(2\psi) - 2) \sin(\theta) \\ &\quad + 0.25 \sin(2\psi) \cos(3\theta) + 0.25 \cos(2\psi) \sin(3\theta) \end{aligned} \quad (32)$$

$$\begin{aligned} \cos(\theta + \psi) \sin^2(\theta) &= 0.25 \cos(\psi) \cos(\theta) - 0.75 \sin(\psi) \sin(\theta) \\ &\quad - 0.25 \cos(\psi) \cos(3\theta) + 0.25 \sin(\psi) \sin(3\theta) \end{aligned} \quad (33)$$

By grouping coefficients, we express the arc-length derivative of normal curvature as a sum of first order and third order sinusoidal functions:

$$\kappa'_n(\theta) = F_{1cos} \cos(\theta) + F_{1sin} \sin(\theta) + F_{3cos} \cos(3\theta) + F_{3sin} \sin(3\theta) \quad (34)$$

where

$$F_{1cos} = 0.25(3A \cos(\psi) - C \sin(2\psi) + D \cos(\psi)) \quad (35)$$

$$F_{1sin} = 0.25(-3A \sin(\psi) + 3B - C(\cos(2\psi) - 2) - 3D \sin(\psi)) \quad (36)$$

$$F_{3cos} = 0.25(A \cos(3\psi) + C \sin(2\psi) - D \cos(\psi)) \quad (37)$$

$$F_{3sin} = 0.25(-A \sin(3\psi) - B + C \cos(2\psi) + D \sin(\psi)) \quad (38)$$

Finally, we can combine the sine and cosine functions to formulate the arc-length derivative of normal curvature as a sum of phase-shifted sinusoidal functions of the angle θ :

$$\kappa'_n(\theta) = F_1 \cos(\theta + \alpha) + F_3 \cos(3(\theta + \alpha + \beta)) \quad (39)$$

where the parameterization independent third order shape parameters can be expressed in closed-form as:

$$F_1 = \frac{\sqrt{F_{1cos}^2 + F_{1sin}^2}}{4}, \quad F_3 = \frac{\sqrt{F_{3cos}^2 + F_{3sin}^2}}{4} \quad (40)$$

$$\alpha = \tan^{-1} \left(\frac{-F_{1sin}}{F_{1cos}} \right), \quad \beta = \frac{1}{3} \tan^{-1} \left(\frac{-F_{3sin}}{F_{3cos}} \right) - \alpha \quad (41)$$

To summarize: in order to compute the third order shape parameters for any point u, v on a general surface patch, we need to compute the parameterization dependent third order (P, Q, S, T) and first order (E, F, G) parameters. Algebraic manipulation of these parameters yields the coefficients ($F_{1\cos}, F_{1\sin}, F_{3\cos}, F_{3\sin}$) of the four sinusoidal components of arc-length derivative of normal curvature. These four coefficients then readily yield the required F_1, F_3, α and β parameters.

7 Qualitative Description of the Fourier Components

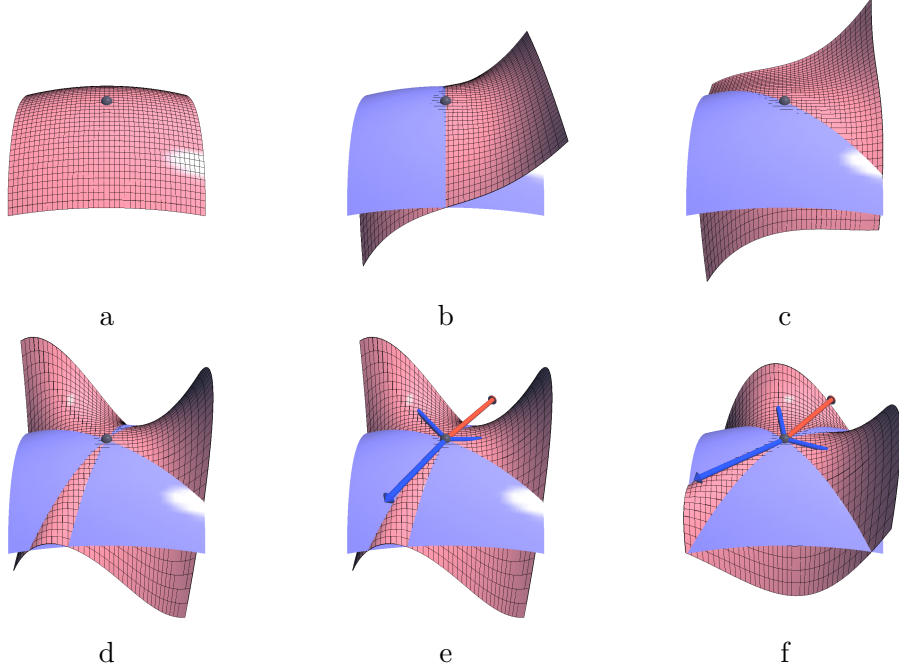


Figure 6: **Sequence of third order shape edits:** Starting from a purely second order surface patch where F_1 and F_3 are zero (a), we increase the amplitude F_1 of the first Fourier component (b), rotate it about the z -axis by increasing the value of α (c), and increase the amplitude F_3 of the third Fourier component (d). (e) shows the same shape as (d) but with the third order frame indicating the directions of α and β . Finally, we rotate only the third Fourier component about the z -axis by increasing the value of β (f). The blue surface is the best-fitting (and unchanged) quadratic surface at the point of analysis.

The shapes of the first and third Fourier components are shown in Fig. 5. Both functions are anti-symmetric with respect to π , which leads to their combination being anti-symmetric as well ($z_{p_c}(r, \theta) = -z_{p_c}(r, \pi + \theta)$) — a fact pointed out separately by Berry and Hannay’s study of umbilics [1] and Mehlum and Tarrou’s study of normal curvature variation [6].

In the range $[0, 2\pi]$, the first Fourier component has one maximum and minimum. The shape of this component is similar to that of the height field $z = x^3 + xy^2$ and can be understood as a lateral extrusion of the cubic curve $z = x^3$ in the y direction, enhanced by a linear component whose slope increases as the square of y (see Fig. 5). When F_1 is zero, the first Fourier component is flat and the angle α cannot be uniquely determined (in this case, we set α to zero). We consider such a point a third order equivalent of the umbilic. Unlike the umbilic where the normal curvature is equal in all directions, at the third order equivalent of the umbilic the normal curvature derivative does not

necessarily behave the same — it is influenced by the non-zero third Fourier component. In fact, as shown by [6], the *only* situation when the normal curvature derivative is equal in all directions is when it is zero, meaning the surface is flat in third order (i.e. both F_1 and F_3 are zero).

In the range $[0, 2\pi]$, the third Fourier component has three equally spaced maxima and minima. The shape of this component is similar to that of the height field $z = x^3 - 3xy^2$. This is the well-known “monkey saddle”, with three peaks and troughs, each $\pi/3$ radians apart. The angle β denotes the rotation of the third Fourier component with respect to the α direction given by the first Fourier component. As shown in Fig. 6, given a fixed α and F_1 , we can vary β and F_3 to change the undulatory behavior of the third order height function. When F_3 is zero, β cannot be uniquely determined, so we set it to zero.

7.1 Expressing Cross Derivatives Using Third Order Shape Parameters

Eqn. 39 gives an expression for the *inline* derivative of curvature (κ'_n) — the change of curvature is analyzed along the line for which normal curvature is measured. Alternately, we can consider *cross* derivatives of curvature (κ_n^\times), where the change of curvature is analyzed in a direction perpendicular to the line along which the normal curvature is measured. For example, Joshi and Séquin [4] introduced the MVS_{cross} functional that contains cross derivative terms in principal directions: $d\kappa_1/de_2$ and $d\kappa_2/de_1$. Here we use our third order parameters F_1 , F_3 , α , and β to obtain an expression for the cross derivative of normal curvature.

Suppose we are given a surface point with normal curvature $\kappa_n(\theta)$ in a direction given by angle θ in the tangent plane. The cross derivative $\kappa_n(\theta)^\times$ is a directional derivative of $\kappa_n(\theta)$ along the direction denoted by $\theta + \pi/2$. We can show that the cross derivative is given by the formula:

$$\begin{aligned}\kappa_n(\theta)^\times &= \frac{F_1}{3} \cos((\theta + \pi/2) + \alpha) - F_3 \cos(3((\theta + \pi/2) + \alpha + \beta)) \\ &= -\frac{F_1}{3} \sin(\theta + \alpha) - F_3 \sin(3(\theta + \alpha + \beta))\end{aligned}\quad (42)$$

The above Eqn. 42 is similar to the Eqn. 39 which expresses the normal curvature derivative (κ'_n) using the third order shape parameters. There are three differences: (1) the F_1 component is reduced to a third of its original value, (2) the F_3 component switches sign and (3) the angles are shifted by $\pi/2$ radians.

The derivation for Eqn. 42 proceeds as follows: we can express the third order surface information at the point of analysis by the idealized cubic height field function, similar to Sec. 3.

$$z(x, y) = C_0x^3 + C_1y^3 + C_2x^2y + C_3xy^2 \quad (43)$$

We can use this description in a small neighborhood around a surface point where the first fundamental form is the identity matrix and the second fundamental form is zero.

Suppose we are interested in the cross derivative $\kappa_{ny}^\times = \frac{d\kappa_n(\pi/2)}{dx} = \frac{d}{dx} \frac{d^2z}{dy^2} = \frac{d^3z}{dy^2 dx} = 2C_3$. We will show how this cross derivative is closely related to the inline curvature derivative $\kappa'_{nx} = \frac{d\kappa_n(0)}{dx} = \frac{d^3z}{dx^3} = 6C_0$.

Consider the situation when F_1 is non-zero and F_3 is zero. Without loss of generality, we can define the x - y coordinate system around such a surface point such that $C_0 = C_3 \neq 0$ and $C_1 = C_2 = 0$ (the x direction is along the maximal direction of the F_1 component). In this case, $\frac{d^3z}{dxdy^2} = \frac{1}{3} \frac{d^3z}{dx^3}$, which implies that the value of the cross derivative of normal curvature is equal to one third the value of the inline derivative of normal curvature, where both curvature derivatives

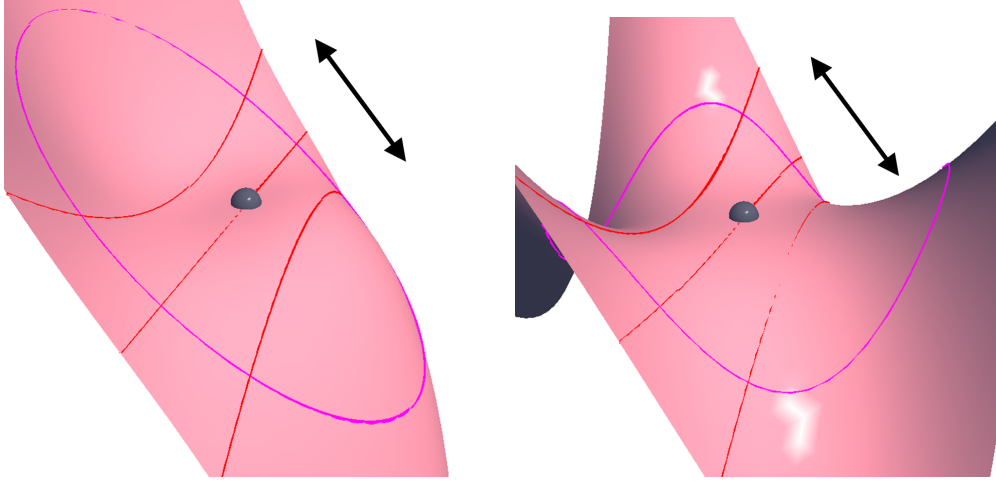


Figure 7: Arrows indicate the directions of maximum cross derivative of curvature for a surface with only (a) F_1 component (single direction of maximum cross derivative) and (b) F_3 component (three directions of maximum cross derivative, each $\pi/3$ radians apart). Notice that along the direction of maximum cross derivative, the curvature of the red curves undergoes maximum change. The directions of high cross curvature derivative correspond to regions of the pink curve (a sample of the surface at a fixed radius) with high curvature.

are in the same direction. For a general direction denoted by θ , the cross derivative in the direction $\phi = \theta + \pi/2$ of the normal curvature $\kappa_n(\theta)$,

$$\frac{d\kappa_n(\theta)}{d\mathbf{e}_\phi} = \frac{1}{3} \frac{d\kappa_n(\phi)}{d\mathbf{e}_\phi} \quad (44)$$

$$= \frac{1}{3} F_1 \cos(\phi + \alpha) = \frac{1}{3} F_1 \cos(\theta + \pi/2 + \alpha) \quad (45)$$

$$= -\frac{1}{3} F_1 \sin(\phi + \alpha) \quad (46)$$

Now consider the situation when F_1 is zero and F_3 is non-zero. Without loss of generality, we can define the x - y coordinate system around such a surface point such that $C_0 = -3C_3 \neq 0$ and $C_1 = C_2 = 0$ (the x axis is along one of the maximal directions of the F_3 component). In this case, $\frac{d^3z}{dxdy^2} = -\frac{d^3z}{dx^3}$ which implies that the value of the cross derivative of normal curvature is equal to the negative value of the inline derivative of normal curvature, where both curvature derivatives are in the same direction. For a general direction denoted by θ , the cross derivative in the direction $\phi = \theta + \pi/2$ of the normal curvature $\kappa_n(\theta)$,

$$\frac{d\kappa_n(\theta)}{d\mathbf{e}_\phi} = -\frac{d\kappa_n(\phi)}{d\mathbf{e}_\phi} \quad (47)$$

$$= -F_3 \cos(3(\phi + \alpha + \beta)) = -F_3 \cos(3(\theta + \pi/2 + \alpha + \beta)) \quad (48)$$

$$= -F_3 \sin(3(\theta + \alpha + \beta)) \quad (49)$$

Just like the inline curvature derivative function κ'_n , we can express the cross curvature derivative function κ_n^\times as a sum of its first and third order Fourier components. By combining the Eqn. 46 and 49, we get the expression for Eqn. 42.

7.2 Expressing Normal Curvature Derivatives in Arbitrary Directions Using Third Order Shape Parameters

The inline and cross derivatives are only two of the infinitely many directions in which we can compute directional derivatives of normal curvature. Given a surface point and a normal curvature $\kappa_n(\theta)$ measured along a direction given by θ , we should be able to compute the directional derivative $d\kappa_n(\theta)/d\mathbf{e}_\psi$ for an arbitrary direction \mathbf{e}_ψ . Note that at any surface point, up to third order, we can define a rank-3 tensor that takes 3 directions as input: two (equal) directions to query the curvature tensor and specify the normal curvature and a third direction to specify the direction of normal curvature derivative (see [9], [3]). We now show that the normal curvature derivatives in all other directions are simple linear combinations of inline and cross curvature derivatives.

Recall the rule of directional derivatives: suppose f is a scalar function over a domain spanned by directions $\hat{\mathbf{x}}$ and $\hat{\mathbf{y}}$. Let the direction \mathbf{m} also be spanned by the x - y basis ($\mathbf{m} = m_x \hat{\mathbf{x}} + m_y \hat{\mathbf{y}}$). Then, the directional derivative $\frac{\partial f}{\partial \mathbf{m}} = \mathbf{m} \cdot (\frac{\partial f}{\partial x} \hat{\mathbf{x}} + \frac{\partial f}{\partial y} \hat{\mathbf{y}})$.

Let the direction of the inline derivative be along the x axis, and the direction corresponding to the cross derivative be along the y axis. A vector along an arbitrary direction given by angle ψ can be written as $\cos(\psi) \hat{\mathbf{x}} + \sin(\psi) \hat{\mathbf{y}}$. Therefore, using the above rule, given the inline and cross derivatives of normal curvature: $\kappa_n(\theta)'$ and $\kappa_n(\theta)^\times$, we can express the directional derivative of $\kappa_n(\theta)$ as:

$$\begin{aligned} \frac{d\kappa_n(\theta)}{d\mathbf{e}_\psi} &= (\cos(\psi) \hat{\mathbf{x}} + \sin(\psi) \hat{\mathbf{y}}) \cdot (\kappa_n(\theta)' \hat{\mathbf{x}} + \kappa_n(\theta)^\times \hat{\mathbf{y}}) \\ &= \kappa_n(\theta)' \cos(\psi) + \kappa_n(\theta)^\times \sin(\psi) \end{aligned} \quad (50)$$

where ψ is computed as the offset angle from the direction of θ .

7.3 Application: Classification of Umbilics

As one example, we show how to use our third order shape parameters to characterize the surface behavior near umbilic points (points with equal principal curvatures). As mentioned before, generic umbilic points on surfaces are classified according to the pattern made by lines of curvature as they pass through the point. Since the surface behavior up to second order is uniform in all directions, we need a third order analysis to classify umbilics. As presented by [1], based on the pattern of lines of curvature near the point, there are three types of generic (stable) surface umbilics: *lemon*, *monstar* and *star* (see Fig. 8). The pattern of lines of curvature depends on the number of real, distinct roots of the cubic equations $z_{pc}(r, \theta) = 0$ (z_{pc} from 3) and $\frac{dz_{pc}(r, \theta)}{d\theta} = 0$. The roots can be obtained by computing the discriminants of the two cubic equations (the third order height function and $\frac{dz_{pc}(r, \theta)}{d\theta} = 0$). Computing the roots is useful if one needs to find the exact location of the lines of curvature, but the discriminants and roots by themselves do not provide a quick geometric understanding of how the surface behaves near the umbilic point. Instead, our third order shape parameters offer a more intuitive explanation of when and how different types of umbilics are formed. When the first Fourier component dominates the overall third order behavior, we get only one maximum and minimum for $z_{pc}(r, \theta)$. In that case, we have the *lemon* type of umbilic. When the third Fourier component is strong enough that its derivatives (slope) exceed those of the first component, we get three distinct maxima and minima (six real roots for the equation $\frac{dz_{pc}(r, \theta)}{d\theta} = 0$) and obtain the *monstar* umbilic. If the third Fourier component dominates the third order height function and creates six zero crossings (instead of two), we get the *star* type of umbilic. Fig. 8 compares the network of curvature lines to the number of zeros and extrema of the third order height function evaluated along a small circle around the umbilic point.

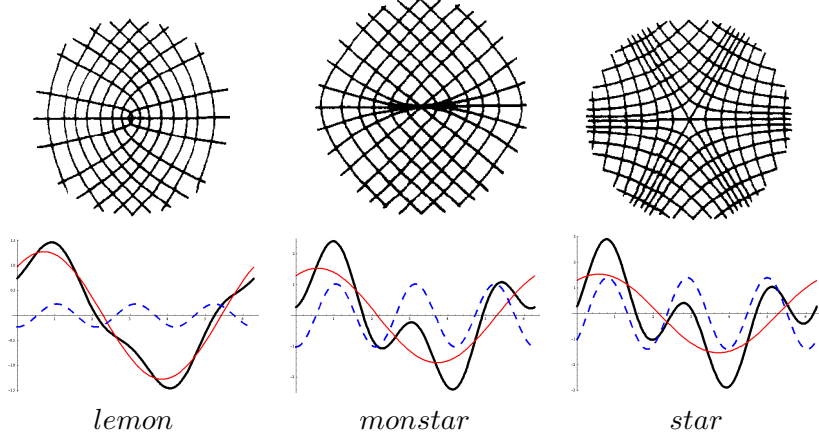


Figure 8: Curvature lines near the three types of umbilic points with the graphs of corresponding third order height functions (thick black). The top row of figures is from [1]. The number of extrema (two or six) and zero crossings (two or six) of the height function together determine the type of the generic umbilic point. Notice how the first Fourier component (red) dominates the overall third order behavior for the *lemon* umbilic, while the third Fourier component (blue) creates local extrema in the *monstar* umbilic and additional zero crossings of the height function in the *star* umbilic.

8 Summary

We have presented an intuitive analysis of third order surface behavior in terms of Fourier components of the third order height function. We hope our exposition will be useful as a tool for studying and characterizing third order geometry. In the next chapter, we will use our understanding of third order surface behavior to define aesthetic functionals built from the fundamental building blocks F_1 and F_3 .

References

- [1] M. Berry and J. Hannay. Umbilic points on gaussian random surfaces. *Journal of Physics A: Mathematical and General*, 10(11):1809–1821, 1977.
- [2] D. DeCarlo, A. Finkelstein, S. Rusinkiewicz, and A. Santella. Suggestive contours for conveying shape. *ACM Transactions on Graphics (Proc. SIGGRAPH)*, 22(3):848–855, 2003.
- [3] J. Gravesen and M. Ungstrup. Constructing invariant fairness measures for surfaces. *Advances in Computational Mathematics*, 17(1):67–88, 2001.
- [4] P. Joshi and C. Séquin. Energy minimizers for curvature-based surface functionals. *Computer-Aided Design and Applications*, 4(5):607–617, 2007.
- [5] T. Maekawa, F. Wolter, and N. Patrikalakis. Umbilics and lines of curvature for shape interrogation. *Comput. Aided Geom. Des.*, 13(2):133–161, 1996.
- [6] E. Mehlum and C. Tarrou. Invariant smoothness measures for surfaces. *Advances in Computational Mathematics*, 8(1):49–63, 1998.

- [7] H. Moreton and C. Séquin. Functional optimization for fair surface design. In *SIGGRAPH*, pages 167–176, 1992.
- [8] I. Porteous. *Geometric Differentiation*. Cambridge University Press, 2nd Edition, 2001.
- [9] S. Rusinkiewicz. Estimating curvatures and their derivatives on triangle meshes. In *Symposium on 3D Data Processing, Visualization, and Transmission*, 2004.
- [10] K. Watanabe and A. Belyaev. Detection of salient curvature features on polygonal surfaces. *Comput. Graph. Forum*, 20(3), 2001.
- [11] G. Xu and Q. Zhang. G2 surface modeling using minimal mean-curvature-variation flow. *Comput. Aided Des.*, 39(5):342–351, 2007.